Magma Redox Geochemistry

Maria Rita Cicconi, Charles Le Losq, Grant S Henderson, Daniel R Neuville

19

The Redox Behavior of Rare Earth Elements

Maria Rita Cicconi[1], Charles Le Losq[2], Grant S. Henderson[3], and Daniel R. Neuville[1]

ABSTRACT

Elements in the lanthanides series are usually known under the name of rare earth elements (REE). In past decades, the use of these elements in industrial processes has increased exponentially with the development of novel technologies and applications. In addition to such growing industrial importance, and despite their relatively low concentrations in the Earth system, REE are sensitive markers of crystal-melt equilibria in geological systems. As a result, the study of lanthanides in materials, either as whole group or as single species, has become an important point of focus in both Geo- and Materials Sciences.

Among REE, Ce and Eu are stable in many geological environments, with two different oxidation states (Ce^{3+}/Ce^{4+} and Eu^{2+}/Eu^{3+}), hence, these two redox couples have been proposed as proxies for oxygen fugacity (fO_2) in different environments (oxybarometer). However, it is essential to understand the factors influencing redox mechanisms in order to use Ce/Eu distribution as fO_2 sensors.

In this chapter, we present an overview of REE properties in minerals, melts, and glasses, and illustrate their importance through examples of applications in the fields of geochemistry, petrology, and mineralogy.

OVERVIEW

"The rare earths perplex us in our researches, baffle us in our speculations, and haunt us in our very dreams. They stretch like an unknown sea before us, mocking, mystifying and murmuring strange revelations and possibilities" (statement attributed to Sir William Crookes, 1902).

The study of trace elements in silicate glasses is a key to understanding the influence of the chemical composition of glasses on the chemical, physical, and rheological properties of a magma. Since the paper of McIntire (1963), trace elements have been widely used as monitors of magmatic processes. But, despite the huge experimental effort devoted to the comprehension of the distribution and behavior of many trace elements in natural systems, our limited knowledge on this topic prevents prediction of magmatic differentiation in most cases.

REE are particularly important in Geosciences and are the most widely used trace elements in geochemical studies of magma genesis. Their distribution in silicate melts/crystals may be used as an indicator of the genetic history of the magma. Indeed, the geochemistry of these trace elements in rocks, glasses, and aquatic systems has been a major research topic for several years, and the REE distribution in these geological settings (on Earth, but not exclusively) has been of great utility in enhancing our understanding of a variety of geological, geochemical, and cosmochemical processes.

[1]*Institut de Physique du Globe de Paris – IPGP, équipe Géomatériaux. 1, rue Jussieu, F- 75005 Paris cedex 05, France*

[2]*Research School of Earth Sciences, the Australian National University, Building 142, Mills Road, Canberra 2601, Australia*

[3]*Department of Earth Sciences, University of Toronto, Toronto, Ontario M5S 3B1, Canada*

Magma Redox Geochemistry, Geophysical Monograph 266, First Edition.
Edited by Roberto Moretti and Daniel R. Neuville.

DOI: 10.1002/9781119473206.ch19

19.1. INTRODUCTION

19.1.1. Trace Elements

A trace element may be defined as an element that is present in a rock at concentration less than 0.1 wt%. Trace elements can form mineral species on their own, but most commonly substitute for major cations in rock-forming minerals. These elements constitute only a small fraction of the system of interest; nevertheless, they provide important geochemical and geological information (Shaw, 2006; White, 2013). This is because:

1. relative variations in the concentrations of many trace elements are much larger than variations in the concentrations of major components;
2. in any system there are far more trace elements than major elements. Each element has chemical properties that are to some degree unique, hence there is unique geochemical information contained in the concentration variation for each element;
3. the range in behavior of trace elements is large, making them sensitive to processes to which major elements are insensitive;
4. trace elements obey Henry's Law, thus their behavior is almost always simpler than that of major elements (White, 2013).

The partition coefficient (D) is the ratio of the concentration of a trace element in a solid phase with respect to that in a liquid at equilibrium, and it is one of the most useful tools to describe magmatic processes (e.g., Bédard, 2006; O'Hara, 1995). The partition coefficient allows distinguishing between compatible and incompatible elements. Incompatible elements are those with $D << 1$ and prefer the melt phase, whereas compatible elements are those with $D \geq 1$ and prefer the mineral phase. Treuil and coworkers (e.g., Treuil & Varet, 1973; Treuil & Joron, 1975; Treuil et al., 1979) proposed another term to further differentiate incompatible elements, and coined the term hydromagmatophile to describe those elements having the highest affinity for the melt phase (Th, U, Zr, Hf, Nb, Ta, REE). The partition coefficient for a given element will vary considerably between different crystalline phases and can be less than one for one phase and greater than one for another. Hence, the terms compatible and incompatible have meaning only when the mineral phases are known. REE are not readily accepted by most silicate minerals, thus they belong to the incompatible elements group.

Incompatible and compatible elements can be divided on the basis of their charge (Z) and size (Figure 19.1a), or in terms of ionic potential (the ratio between charge and ionic ratio). Another parameter was proposed by Dietzel (1948): the Cation Field Strength CFS = $Z/(r_c+r_O)^2$, where Z is the charge of the cations and the denominator represents the cation- oxygen distance (here considered oxygen ionic radius =1.35 Å) (Figure 19.1b).

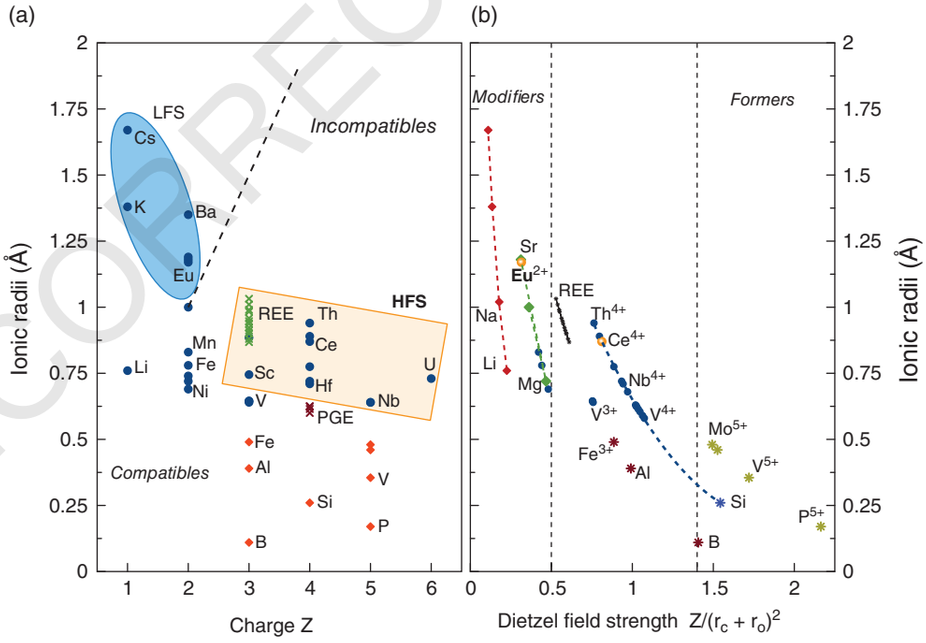

Figure 19.1 (a) Plot of ionic radius (data from Shannon, 1976) vs. ionic charge for trace elements of geological interest. Red diamonds refer to four-fold coordinated cations (modified after Rollinson, 1993). (b) Dietzel's field strength parameter for several cations (stars refer to four-fold coordinated cations).

Figure 19.1a shows a plot of ionic radii against charge for several trace elements, here considered six-fold coordinated. Small highly charged cations are known as high field strength (HFS) cations (e.g., Hf^{4+}, Th^{4+}, Ce^{4+}, Ta^{5+}, U^{6+}) and large cations of small charge are referred as low field strength (LFS) cations (Ba^{2+}, Eu^{2+}, Sr^{2+}, Pb^{2+}, K^{+}). LFS cations are also known as large ion lithophile elements (LILE). Elements with small ionic radius and a relatively lower charge tend to be compatible, and the most common four-fold coordinated network-forming cations are reported as red diamonds (Figure 19.1a). Figure 19.1b shows the relationship between the Dietzel's field strength and the ionic radii (six-fold coordinated cations) for several elements. It is similar to the charge vs. ionic radii plot, but it further shows the grouping of cations based on their structural role. Indeed, according to Dietzel (1948), the field strength is a critical parameter for glass formation, with network-forming cations having high field strength values (> 1.3–1.4), whereas network modifiers have low field strengths (< 0.5).

The two plots in Figure 19.1 highlight the main groupings of trace elements and emphasises the similarity in ionic size and charge between some elements/groups. Elements with the same ionic charge and size are expected to show very similar geochemical behaviour (Rollinson, 1993).

19.1.2. Lanthanides

The lanthanide series includes 15 elements of the periodic table (from Lanthanum to Lutetium), and they are also called rare earth elements (REE). However, often "rare earth" has been applied in a more unrestricted way, thus including Sc and Y.

Lanthanides have a $5d^1\ 6s^2$ outer electron orbital arrangement. With increasing atomic number, the inner *4f* shell is filled before the second *5d* electron shell get filled (thus lanthanides belong to the 3B group of the periodic table) and the similarity in their chemical properties is the result of their atomic structure. Lanthanides might be considered as a separated group from the rest of the periodic table, if the main interest is related to the properties that depend on the occupancy of the *4f* electron shell, from 0 (La) to 14 (Lu) (Figure 19.2).

Figure 19.2 shows the dependence of the six-fold coordinated $^{[6]}REE^{3+}$ ionic radii in going from La to Lu (data from Shannon, 1976). Moving from left to right across the periodic table (increasing atomic number), the radius of each lanthanide 3+ ion gradually decreases, and this is referred to as "the lanthanide contraction" and it is caused by the poor screening of the *4f* electrons. Beside the values for trivalent lanthanides, the ionic radii for Ce and Eu in different oxidation states are also reported in Figure 19.2. Indeed, those elements are multivalent, and their

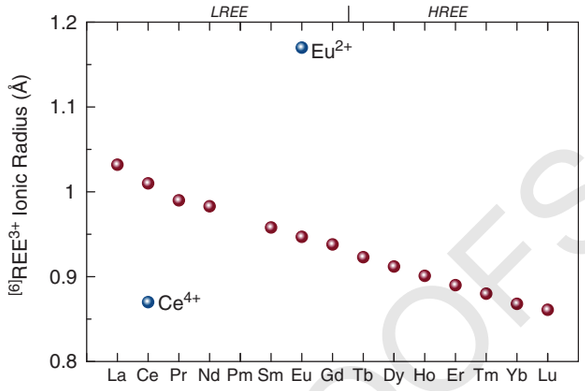

Figure 19.2 Ionic radii for six-fold coordinated REE^{3+}. (Radius values from Shannon, 1976).

electronic state in melts and minerals is determined by temperature as well as the redox state of the system[1]. Multivalent REE are stable in the trivalent state over a wide range of oxygen partial pressures. Nevertheless, at the oxygen fugacity (fO_2) of the Earth's surface Ce can be stabilized partly or entirely in the tetravalent state and Eu can be partly stabilized in the divalent state at lower oxygen fugacities (e.g., Earth's interior) (White, 2013).

REE are divided into light and heavy groups based on their atomic weight. The light rare earth elements (LREE) are, usually, from La to Gd, whereas the heavy rare earth elements (HREE) are from Tb to Lu. Because of their relative high charge and large ionic radius, the lightest REE are considered highly incompatible (Figure 19.1), whereas the heavy REE have appropriately small radii and might be accommodated in many common minerals (e.g., garnets in Figure 19.3).

The REE are typically not readily accepted by most petrogenetically important silicate minerals but can be compatible in a few major minerals. According to McKay (1989) the importance of REE for petrogenetic modeling mainly arises from four factors:

1. Their ionic radii vary systematically with atomic number. Hence, because of the strong influence of size on partitioning, REE partition coefficients also vary smoothly with atomic number. On the other hand, the shapes of the partition coefficient patterns (plots of distribution coefficient versus atomic number) are very different from one mineral to another.

2. The systematic variation of the REE partition coefficients with atomic number sometimes presents spikes related to the so-called Eu-(Ce) anomalies. Indeed, beside the trivalent state typical of REE, Ce can be partly or

[1] In this chapter, we use oxygen fugacity, fO_2, as equivalent of the partial pressure of oxygen.

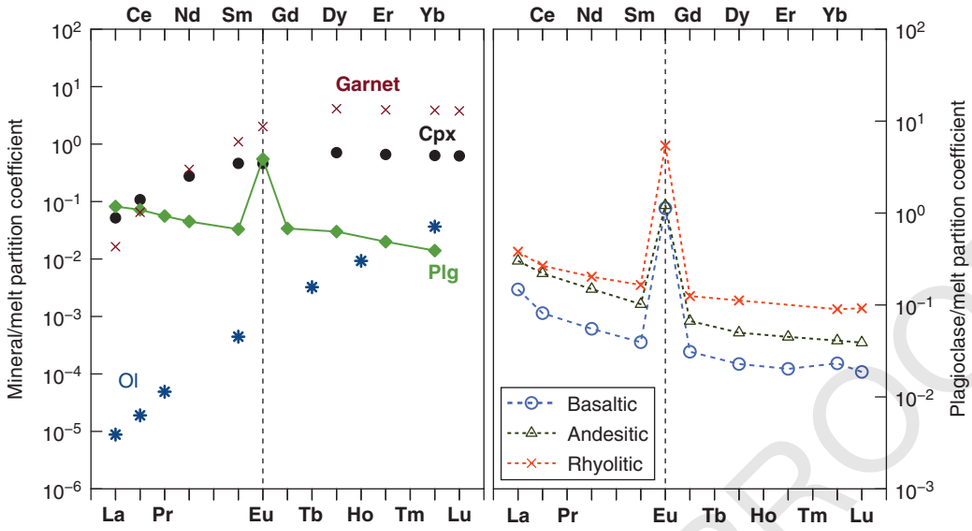

Figure 19.3 (a) Mineral/melt REE partition coefficients for plagioclase (Plg), olivine (Ol), clinopyroxene (Cpx), and garnet in basaltic melts. (b) REE plagioclase/melt partition coefficients in basalt, andesite, and rhyolite. Data compilation from Rollinson (1989) and references therein.

entirely stabilized in the oxidized form (Ce^{4+}) and Eu can be partly stabilized in the reduced form (Eu^{2+}) (Figure 19.2). The latter especially has been considered strongly diagnostic of the involvement of certain minerals in petrogenetic processes.

3. Since REE are highly refractory elements, their relative abundances, in most undifferentiated materials, are generally assumed to be proportional to their relative abundances in the sun and in chondritic meteorites. Thus, they minimize one of the free parameters in most petrogenetic models: the relative elemental abundances in the starting material (cf. McKay, 1989).

4. There are three important isotopic systems that provided a major contribution in the understanding of planetary evolution processes: Sm-Nd, Lu-Hf, and La-Ce.

19.2. GEOCHEMISTRY OF RARE EARTH ELEMENTS

The determination of the partition coefficient between coexisting phases (i.e., mineral/melt) is essential for using REE partition coefficient patterns in the understanding of magmatic differentiation. REE abundance, in natural minerals and magmas follows the Oddo-Harkins rule: a lanthanide with even atomic number is more abundant than its neighboring lanthanides with odd atomic numbers. Normalizing the REE abundances to those in chondritic meteorites is usually performed as it eliminates effects related to nuclear stability and nucleosynthesis, and further produces a smooth pattern (White, 2013). CI chondrites are a class of meteorites that are taken to be the best representative of the average concentrations of non-volatile elements in the solar system.

The mineral/melt REE partition coefficient patterns in the major minerals involved in basaltic magma petrogenesis are reported in Figure 19.3a. The partition coefficient patterns are similar in basaltic, andesitic, and rhyolitic liquids. However, differences of one to several orders of magnitude, in the absolute values, can be observed. Even when comparing the mineral/melt REE partition coefficient data for a synthetic lunar mare basalt (e.g., Lipin & McKay, 1989) it is possible to observe comparable trends. Hence, there is a strong chemical control on the REE partitioning. Olivine (Ol in Figure 19.3a) produces little REE fractionation in partial melts, and the pattern increases from LREE to HREE. For garnet/melt partition coefficient the pattern slopes upward as well, as HREEs enter into Al sites in garnets.

Comparing partition coefficient values for pyroxenes reported in the literature is quite challenging because they vary between published sources, indicating that pyroxene patterns are strongly dependent on composition. For example, McKay (1989) reported that a low-Ca (pigeonite) and a high-Ca pyroxene (augite) present quite different trends. Furthermore, Gaetani and Grove (1995) observed that the proportion of Al entering a pyroxene influences the Ce and Yb partition coefficients between clinopyroxene and melt.

The plagioclase/melt REE partition coefficients form a pattern quite different compared to that of the other minerals (Figure 19.3a). The pattern decreases from

LREE to HREE and the value of REE partition coefficients are generally low, with one exception: Eu. Indeed, the partition coefficient for Eu in plagioclase (D_{Eu}) is anomalously higher compared to the other REE. This exception is referred to as the "Eu-anomaly," and greater values of D_{Eu} are called positive anomalies. The positive Eu-anomaly in the plagioclase/melt partition coefficients means that a significant proportion of europium is entering in the crystal. Indeed, the reduced species Eu^{2+} enters the large alkali/alkali-earth site in the plagioclase structure. Figure 19.3b shows the plagioclase/melt partition coefficients for the REE vs. atomic number, respectively for basaltic, andesitic, and rhyolitic compositions. In addition to the mineral phase, the composition of the melt influences REE partition coefficient patterns. By increasing the silica content (and polymerization) of the melt, there is a clear increase in the REE partition coefficients, with almost one order of magnitude difference between basalt and rhyolite melts (Figure 19.3b).

The ionic radius of reduced europium ($^{[6]}Eu^{2+}$ = 1.17 Å) is much larger than that for trivalent europium ($^{[6]}Eu^{3+}$ = 0.947 Å; ionic radii from Shannon, 1976) (Figure 19.2). Combined with the difference in charge, this produces large variations between Eu divalent and trivalent partition coefficients in many minerals.

Based on Figure 19.1, a strong correlation between coordination and ionic radius is clear, and larger cations likely will occupy larger sites in minerals, and vice versa. Onuma et al. (1968) noted that for any particular mineral, partition coefficient values, when plotted with respect to the cation ionic radii, tend to lie along convex-upwards curves, with a different curve for each valence. Furthermore, each curve tends to parallel those for ions of different valences, with the maximum occurring at the same ionic radius for each valence. Based on these observations, Onuma et al. (1968) concluded that (i) trace elements preferentially occupy lattice sites rather than occurring as defects or as inclusions; (ii) for trace elements of the same charge, the difference between the ionic radius of the trace ion and that of the major element being substituted for, exercises the dominant control on the partition coefficient; and (iii) the effect of ionic charge on partition coefficients appears to be independent of the effect of ionic radius.

One can note that REE^{3+} partitioning could be well predicted by using a valence versus ionic radii plot, as shown in Figure 19.1a.

19.3. MULTIVALENT RARE EARTH ELEMENTS

19.3.1. Europium

Considering that the charge of trace cations influences their ionic radius, changes in their oxidation state can produce marked variations in partitioning behavior. Among the REE, Eu is the only element for which a significant proportion of the ions, in igneous systems, are likely to be present in valences other than trivalent. This leads to "anomalous" concentrations of Eu in many igneous systems. As reported, plagioclase is often anomalously rich in Eu compared to the other rare earths and this leads to pronounced positive Eu-anomalies in plagioclase/melt partition coefficient patterns (Figure 19.3b).

Since the proportion of Eu^{2+} and Eu^{3+} are influenced by the prevailing oxygen fugacity (fO_2) conditions, the presence of positive (or negative) Eu anomalies has been considered strongly diagnostic for the understanding of the evolution of petrogenetic processes (McKay, 1989). Thus, understanding the factors influencing europium redox mechanisms is very important, especially when considering using Eu geochemical behavior as a proxy for the oxygen fugacity of the environment (e.g., Papike et al., 2005; Wadhwa, 2008). Consequently, several experimental studies have been carried out on the effect of Eu partitioning as a function of fO_2 (e.g., Drake & Weill, 1975; Philpotts, 1970; Schnetzler & Philpotts, 1970; Weill & Drake, 1973). However, it has been demonstrated that chemistry also plays a key role in influencing the $Eu^{2+}/(Eu^{2+} + Eu^{3+})$ redox ratio in geological materials (e.g., Cicconi et al., 2012; Lauer & Morris, 1977; Müller & Muecke, 1984; Morris & Haskin, 1974).

In the following, we will review the parameters mostly affecting Eu redox state: bulk chemistry, temperature, and fO_2.

As Eu^{2+} and Sr^{2+} cations have identical charge and almost identical ionic radii, Philpotts (1970) suggested that the partitioning of Sr would be equivalent to that of divalent Eu ($D_{Eu^{2+}}$), whereas to obtain the Eu^{3+} partition coefficient ($D_{Eu^{3+}}$) the value could be interpolated from the values of neighbour Sm and Gd. Based on these assumptions, Philpotts (1970) estimated the Eu^{2+}/Eu^{3+} redox ratio in several phases, and proposed Eu partitioning to be used as an oxygen fugacity barometer. Following the approach of Philpotts (1970), the mineral/melt partitioning of Eu under different redox conditions has been studied, for instance, for plagioclases (e.g., Drake & Weill, 1975; Weill & Drake, 1973; Wilke & Behrens, 1999), diopside (Grutzeck et al.1974), and pyroxenes (Ching-oh et al., 1974; Shearer et al., 2006), either in terrestrial, meteorites, or lunar materials. For example, Drake (1975) experimentally studied the partitioning of Eu between plagioclase and magmatic liquid of basaltic and andesitic compositions as a function of temperature and oxygen fugacity conditions. By using the approach of Philpotts (1970), the ratios of divalent and trivalent europium were estimated both in plagioclase minerals and coexisting magmatic liquids. The author showed that the Eu anomaly (Figure 19.4) increases as fO_2 decreases, suggesting that

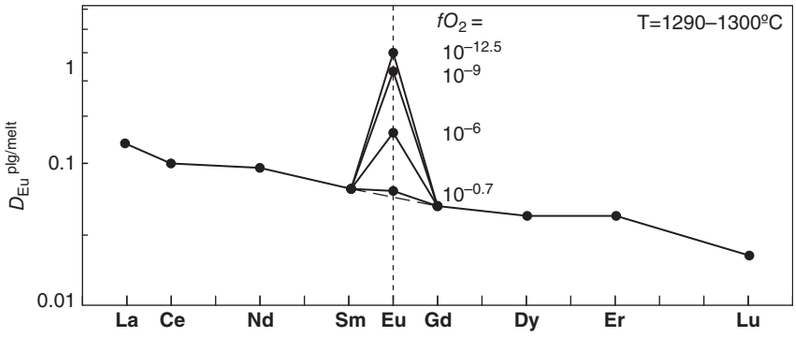

Figure 19.4 Experimental data from Drake (1975) show that the partitioning of Eu between plagioclase feldspar and magmatic liquid ($D_{Eu}^{plg/melt}$) is a strong function of oxygen fugacity conditions. Redrawn after Drake and Weill (1975).

the Eu-anomalies, and in turn, the Eu^{2+}/Eu^{3+} redox ratios in rock-forming minerals, might be used to estimate oxygen fugacity conditions.

The europium redox equilibrium can be expressed as

$$4Eu_{melt}^{3+} + 2O_{melt}^{2-} \leftrightarrow 4Eu_{melt}^{2+} + O_2, \qquad (19.1)$$

where the oxidized Eu^{3+} and reduced Eu^{2+} species and the physically dissolved oxygen of the melt, are in equilibrium. The equilibrium constant K is given by:

$$K = \frac{a\left(Eu_{melt}^{2+}\right)^4 * a(O_2)}{a\left(Eu_{melt}^{3+}\right)^4 * a\left(O_{melt}^{2-}\right)^2}, \qquad (19.2)$$

where K is controlled by oxygen fugacity and the activities (a) of oxygen and europium ions in the melt. Assuming that ionic activities are equal to 1, Equation 19.2 can then be rewritten as

$$-\log(fO_2) = 4\log\left[\frac{Eu^{2+}}{Eu^{3+}}\right] + b, \qquad (19.3)$$

where the square brackets [] denote activity and f denotes fugacity (log is to base 10). b is a term that incorporates all quantities that are function of temperature and bulk chemistry (*cf*. Schreiber, 1987). Equation 19.1 implies the release of 4 electrons during the oxidation of Eu^{2+}, explaining the coefficient 4 visible in Equation 19.3. As a result, a plot of $-\log(fO_2)$ against $\log[Eu^{2+}/Eu^{3+}]$ should provide a slope of 4/1 (for one-electron couples), when samples have the same composition and are produced at the same temperature. However, deviations from the ideal slope have been observed for Eu redox ratios (Morris et al., 1974; Cicconi et al., 2012), as well as for other multivalent elements (e.g., Paul & Douglas, 1965a, b; Schreiber et al., 1999; Cicconi et al., 2015). A possible explanation for deviations from the ideal values can be ascribed to non-equilibrium conditions between liquid and equilibrating gases (Johnston, 1964; Johnston, 1965). On the other hand, the chemical equilibrium reported above is a simplified form, because ions, logically, occur in melt as solvated species coordinated to oxygens within the silicate glass network (Schreiber, 1987). Ergo, the europium ions activities in the melt may not be directly proportional to the concentration redox ratio. In order to obtain the dependence of the redox ratio to the bulk chemistry, Schreiber proposed an alternate form of the chemical equation for redox equilibria by taking into account the number of oxygen associated with the oxidized redox ion in the melt (coordination spheres). Thus, the cation coordination, or more generically speaking, the cation speciation might be a crucial point when studying redox equilibria.

We can summarize that the main parameters that must be taken into account for determining the redox equilibria in melts are:

- the oxygen partial pressure in the melt (i.e., oxygen fugacity at ambient pressure);
- the thermodynamic equilibrium constant, which depends on temperature and standard free energy of the reaction;
- the activities (a) of ions in the melt.

Schreiber et al. (1994) described the dependence of the redox equilibria for several multivalent elements (including Eu and Ce) in simplified sodium silicate compositions, reporting a good correlation with the basicity of the melt. The optical basicity (Λ) concept was firstly introduced by Duffy and Ingram (Duffy & Ingram, 1971, 1976; Duffy, 1993) and developed in the following years by, e.g., Lebouteiller and Courtine (1998), Moretti (2005), and Ottonello et al. (2001). The optical basicity concept has been developed for quantitative determination of the acid–base properties of mixtures containing a large number of oxides, as for instance glasses, alloys, slags, and molten salts. The optical basicity value is obtained from

measurements involving the electron donor power of probe oxides (such as Pb^{2+}). The red shift in the optical absorption band related to the electronic transition 6s $\rightarrow$ 6p is correlated to the increases of covalency, therefore providing the average electron density. For multicomponent systems, such as glasses and melts, the theoretical optical basicity can be calculated by using partial Λ values of oxide components and their molar proportion (Duffy & Ingram, 1976; Duffy, 1993; Lebouteiller & Courtine, 1998; see Le Losq et al., Chapter 12, this volume).

Many multivalent element redox equilibria follow the general rule of redox controlled by melt basicity, with the oxidation-reduction equilibrium shifting toward more oxidized species with increasing basicity of the melt (i.e., by increasing the amount of network-modifying oxides). Since a greater network-modifying ion activity results in increasing melt depolymerization, this parameter can be broadly related to the ratio of non-bridging oxygens (NBO) per tetrahedral cations (T) in glasses and melts (NBO/T parameter).

The dependence of the Eu^{2+}/Eu^{3+} ratio on glass/magma composition, temperature, and redox conditions has been experimentally investigated by using several techniques: Electron Paramagnetic Resonance (EPR), Voltammetry, Optical Absorption and Luminescence Spectroscopy, Mössbauer, and more recently X-Ray Absorption Spectroscopy (XAS).

EPR spectroscopy data (e.g., Lauer & Morris, 1977; Morris & Haskin, 1974; Morris et al., 1974; Schreiber, 1987) confirmed that oxygen fugacity, temperature, and composition are all important parameters that affect the Eu^{2+}/Eu^{3+} redox ratio in melts. This technique was extensively used to evaluate the Eu redox ratios in glasses, though its use is inadequate for natural samples since the presence of iron overshadows/alters the signal related to europium. In addition, the presence of titanium is also problematic for EPR measurements, because the Ti^{3+} signal partially overlaps the Eu^{2+} signal (Lauer & Morris, 1977).

Morris & Haskin (1974) investigated by EPR the dependence of the concentration ratio of Eu^{2+} to Eu^{3+} on bulk chemistry in Ca-Mg-Al silicate melts. The authors determined that Eu^{2+}/Eu^{3+} redox ratio increases with the [(Al+Si)/O] molar ratio, i.e., with decrease in NBO. In a following study, Morris et al. (1974) studied the Eu^{2+}/Eu^{3+} redox ratio in Ca-Mg silicate and Ca-Al silicate glasses depending on temperature and oxygen fugacity conditions. The authors confirmed the endothermic nature of the chemical equation for europium redox equilibrium. For diopsidic and anorthitic compositions they further reported deviations from the ideal slope of 4 (from Equation 19.3) in the $-\log(fO_2)$ vs. $\log [Eu^{2+}/Eu^{3+}]$ plot. On the contrary, Virgo et al. (1981) reported a slope very close to the ideal one for diopside glass composition. Diopsidic composition was studied also via Linear Sweep Voltammetry (LSV) by Colson et al. (1990). This technique was used to measure Eu redox potentials, providing an enthalpy of reduction for Eu^{3+} of 31±5 kcal/mol. Moreover, the authors determined the Eu diffusion rate in diopsidic melt ($1.5E^{-6}$ cm^2/s at 1500 °C).

Additional studies of Eu redox ratios have been performed using Mössbauer spectroscopy (e.g., Concas et al., 1998; Virgo et al., 1981). This technique is useful for the determination of Eu oxidation states since the isomer shift differs significantly between Eu^{3+} and Eu^{2+}. However, it does not allow a precise determination of the occupancy/mixing on the europium sites (Harmening et al., 2010). Using Mössbauer, Virgo et al. (1981) reported that the Eu^{2+}/Eu^{3+} redox ratio decreases by a factor of 4 upon replacement of alkali by alkaline-earth elements in a diopside-like melt composition. Concas et al. (1998) carried out Mössbauer investigations of rare earth sites in europium-bearing glasses of different compositions (phosphate, borate, and silicate). They observed that there is a deviation of the Eu^{3+} sites from cubic symmetry. Thus, the different glass networks influence the Eu^{3+} local environment.

Photoluminescence spectroscopy has been extensively used to study Eu-bearing materials, and in particular the effect of bulk composition on luminescence properties (e.g., Cicconi et al., 2017; Wang et al., 2007). However, most of these studies concern synthetic glasses, glass-ceramics, and crystals for technological applications (e.g., phosphors and LEDs). For geological materials, the photoluminescence techniques have mainly been used for detecting divalent and trivalent Eu in minerals (Gaft et al, 2015). Even if this technique has a high sensitivity (ideal to study trace elements), and is extremely sensitive to variations in the surrounding ligands, it does not allow for quantification of the $Eu^{2+}/(Eu^{2+} + Eu^{3+})$ ratios.

XAS has been used to quantify the Eu^{2+}/Eu^{3+} redox ratio in many minerals because of the high sensitivity and spatial resolution of this technique (Brugger et al., 2006; Rakovan et al., 2001; Shearer et al., 2011; Sutton et al., 2005; Takahashi et al., 2005; Tanaka et al., 1995). This technique has also been recently used on natural and synthetic glasses. Karner et al. (2010) studied the partitioning of Eu between augite and melt, in analogues of martian basalts, as a function of fO_2 (from FMQ to IW-1) [2]. The REE partition coefficients patterns between melt and pyroxenes represent well the different imposed fugacities used for the experiments, with increasing negative Eu anomalies (Karner et al., 2010). The quantification of the Eu^{2+}/Eu^{3+} redox ratio either in residual glass or mineral was obtained by analysis of the X-ray

[2] respectively, Fayalite-Magnetite-Quartz and Iron-Wüstite buffer.

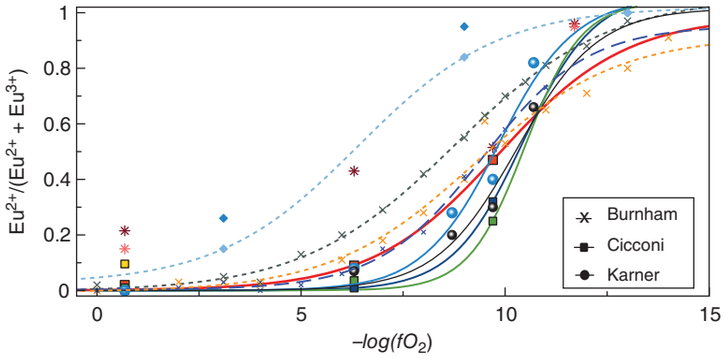

Figure 19.5 $Eu^{2+}/(Eu^{2+} + Eu^{3+})$ redox ratio as determined by XANES vs. oxygen fugacity values, for different bulk compositions. Solid lines represent the evolution of Eu redox ratio with fO_2, extrapolated from data reported by Karner et al. (2010) and Cicconi et al. (2012). Other compositions are haplogranitic glasses (stars; Cicconi et al. 2012) or CAS, MAS compositions (diamonds; Burnham et al., 2015). Crosses (and dotted lines) represent modified diopside-anorthite compositions from Burnham et al. (2015) (AD and AD+qz). Blue dashed line follows the trend of Eu redox in a synthetic MORB glass. See text for details.

Absorption Near Edge Structure (XANES) portion of the XAS spectra. The authors reported that, at the FMQ buffer, europium is mostly present in its oxidized form, both in the melt and in the augite crystal, whereas under more reduced conditions (IW-1) both phases are extremely enriched in reduced europium (circles in Figure 19.5).

Cicconi et al. (2012) synthetized six set of anhydrous glasses with compositions spanning from simplified (Na-silicate) to multicomponent ones resembling haplobasaltic (diopside-anorthite, DiAn) and haplogranitic (HPG8) melts. The authors observed that in glasses synthetized in air the $Eu^{2+}/(Eu^{2+} + Eu^{3+})$ redox ratio markedly increased in going from basaltic to granitic composition (respectively, squares and stars in Figure 19.5), varying from 0.0 up to 0.22 (±0.06). Moreover, Cicconi and coauthors (2012) reported that, in three basaltic compositions equilibrated at 1400 °C under oxygen fugacity conditions close to the FMQ buffer, the Eu oxidation state has only slight variations, with Eu^{3+} still being the predominant species. Only at more reducing conditions (IW buffer), was there evidence of a significant increase in divalent Eu in mafic compositions (squares in Figure 19.5). These observations were in agreement with the previous study of Karner et al. (2010). Felsic samples (haplogranitic glasses; stars in Figure 19.5) always stabilized higher amounts of divalent Eu species. Despite the strong variation of the Eu redox ratio as a function of the bulk melt chemistry, and the correlation between Eu redox state and melt polymerization, Cicconi et al. (2012) suggested that there is not a simple relationship with simplified chemical parameters, such as the non-bridging oxygen per tetrahedron (NBO/T) parameter, the alkali content or the Na/(Na+K) molar ratio. Hence, the dependence of the Eu^{2+}/Eu^{3+} ratio on glass/magma composition might be controlled by a combination of several factors.

Burnham et al. (2015) extended the dataset previously reported on Fe-free, alkali-free Ca-Mg aluminosilicate melts with experiments covering a very wide range of fO_2 (from FMQ-13.7 to FMQ+6.3). Moreover, the authors also reported the data for a synthetic Mid-Ocean Ridge Basalt (MORB). Using this extended set of compositions and oxygen fugacities, the authors corroborate all previous findings, with the $Eu^{2+}/(Eu^{2+} + Eu^{3+})$ redox ratio varying systematically with imposed fO_2 conditions and synthesis temperatures, as well as with melt composition. In Figure 19.5, points related to two diopside-anorthite compositions (AD and AD+qz, equilibrated at 1400 °C) from Burnham et al. (2015) are reported (crosses in Figure 19.5) along the MORB glasses (blue dashed line). Moreover, two compositions in the ternary systems CAS and MAS ($CaO\text{-}Al_2O_3\text{-}SiO_2$ and $MgO\text{-}Al_2O_3\text{-}SiO_2$, respectively) are shown as well (diamonds in Figure 19.5). Interestingly, the values obtained by Burnham and coauthors (2015) for the latter two compositions approach the trend reported by Cicconi et al. (2012) for haplogranitic glasses.

All studies cited above agree on the strong influence of bulk composition on the Eu redox ratio which could be partially rationalized in terms of the influence of the degrees of covalency of the cations building the glass network.

The dependence of Eu redox ratio as described by Morris and Haskin (1974) (on the dependence of Eu redox on melt polymerization and on the increases of the Eu^{2+}/Eu^{3+} as the radius of the network-modifying cation decreases) has been interpreted by Fraser (1975) in terms of the

amphoteric character of europium oxides in silicate melts, and the occurrence of different structural units. Thus, Eu_2O_3 may be seen either as basic or acidic oxide, with two possible reactions occurring in silicate melts (Fraser 1975):

$$Eu_2O_{3\ melt} + O^{2-}_{melt} \leftrightarrow 2EuO^{-}_{2\ melt} \quad (19.4)$$

$$Eu_2O_{3\ melt} \leftrightarrow 2Eu^{3+}_{melt} + 3O^{2-}_{melt} \quad (19.5)$$

The formation of a structural unit, and the acidic or basic nature of the oxide imply that O^{2-} may occur either as product or reactant (similarly to what observed for Fe-S interaction in silicate melts; Moretti & Ottonello, 2003), thus explaining the dependence on the oxide ion activity.

The structural unit EuO_2^- should have an independent geometry site that does not implicate a different structural role in the silicate network. Indeed, taking into account the Dietzel's Cation Field Strength parameter for divalent and trivalent europium (see Figure 19.1b) it is unlikely for Eu^{3+} to behave as a network-former cation. Experimental evidence for the structural role of both trivalent and divalent europium in silicate glasses of geological interest have been provided by EXAFS (Extended X-Ray Absorption Fine Structure) spectroscopy (Cicconi et al., 2012). This study confirmed that Eu ions will behave as network-modifying cations in silicate melts and that they are coordinated with 6 to 9 oxygens (respectively for Eu^{3+} and Eu^{2+}), in agreement with the coordination suggested by Morris & Haskin, 1974, and field strength considerations.

19.3.2. Cerium

Cerium may be stabilized in glasses, melts, and rocks either as Ce^{3+} or Ce^{4+}, and Ce-anomalies (deviations to the general trend) have been detected in several geological systems (terrestrial and lunar rocks, meteorites, minerals, seawater…) and proposed as a redox proxy (e.g., Ballard et al., 2002; Elderfield & Greaves, 1981; Evensen et al., 1978; Masuda et al., 1974; Takahashi et al., 2002; Tostevin et al., 2016; Trail et al., 2011). Indeed, as previously reported for europium, and in general for many multivalent elements (e.g., Cr, V; Papike et al., 2005) the element partitioning between coexisting phases might reflect the average oxygen fugacity conditions at the time of crystallization.

Drake & Weill (1975) observed that the behavior of Ce (as $Ce^{3+} + Ce^{4+}$) does not differ significantly from the value of Ce^{3+} obtained by linear interpolation between the values of La^{3+} and Nd^{3+}. This implies that the partition coefficient of the trivalent species ($D_{Ce^{3+}}$) approximates that of the tetravalent one ($D_{Ce^{4+}}$), resulting in $D_{Ce^{3+}} \sim D_{Ce^{4+}}$ in plagioclase/magmatic liquid systems. More recently, Ballard et al. (2002) determined the Ce^{4+}/Ce^{3+} ratio in zircons and used it to infer the relative oxidation state of calc-alkaline intrusions (associated with porphyry copper mineralization) at the time of crystallization. The authors' method was based on the approach of Philpotts (1970) for europium (see Section 19.3.1). Many following studies were focused on the partitioning of Ce (and on Ce oxidation state) into zircon ($ZrSiO_4$) in order to establish the prevailing redox conditions. Zircons are widespread accessory minerals physically and chemically stable, hence they are considered to preserve the original chemistry (Ballard et al., 2002; Trail et al., 2011).

Ce^{4+} is highly compatible in $ZrSiO_4$, much more than Ce^{3+} (like Hf^{4+}, Th^{4+}; see Figure 19.1) such that its high partitioning into the crystals could indicate highly oxidizing conditions in the melt at the time of crystallization. The occurrence of Ce^{4+} in zircons is emphasised by the positive Ce anomalies. However, as in the case of europium in plagioclase, it is important to obtain a quantitative understanding of the influence of bulk composition, fO_2 conditions and synthesis temperatures on the cerium redox ratio. In the following we report a brief review of the experimental studies carried out in order to assess the effect of several parameters (chemistry, temperature, fO_2) on the Ce redox state.

Earlier investigations used chemical titration for evaluation of Ce redox ratio in glasses. Johnston (1965) estimated the Ce^{3+}/Ce_{tot} redox ratio to vary, in air, from 0.26 at 1000 °C to 0.40 at 1300 °C, from experiments on Ce^{3+}-Ce^{4+} oxidation- reduction equilibria in a binary $Na_2Si_2O_5$ melt. Moreover, the author studied the Ce redox ratio in glasses synthetized at 1085 °C under different fO_2 conditions, reporting the equilibrium dependence of log $[Ce^{3+}/Ce^{4+}]$ on -log(fO_2) with values very close to the theoretical slope of 4.

Paul & Douglas (1965a) also investigated the Ce^{3+}-Ce^{4+} redox equilibria in air, in simple binary borate and alkali silicate glasses. The main goal of this study was to understand the influence of cerium content, alkali cation type, and synthesis temperature on redox. The main results obtained by Paul and Douglas for alkali silicate glasses, synthetized in air, are shown in Figure 19.6, where it is possible to appreciate how the bulk composition affects the Ce redox ratio. In going from Li to K (increasing cation ionic radii), at equal amounts of alkali content, there is an increase of the oxidized species. However, this trend is not linear since the slope of the lines increases in the order Li < Na~K. Similar changes in slope with different alkali cation type were also reported for Fe and Cr redox pairs (Paul & Douglas, 1965b). By increasing the amount of network modifiers (increasing melt basicity) there is a marked increase of the oxidized species for K- and Na-silicate glasses and smaller increases for Li-silicate glasses (Figure 19.6). Further observations by Paul and Douglas (1965a) for alkali borate glasses regard the variation of the Ce redox ratio with the total amount of cerium, and

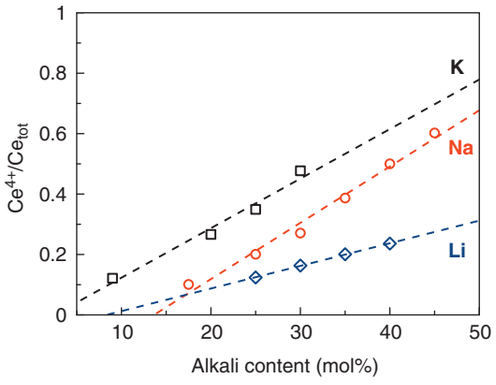

Figure 19.6 Dependence of the Ce^{4+}/Ce_{tot} redox ratio on alkali content, and alkali cation type. Lines are only guide for the eyes. Data from Paul and Douglas (1965) for synthesis in air, at 1400 °C. Errors not provided.

the increase of Ce^{4+} species with gradual increase of cerium concentration. Finally, the effect of temperature was also evaluated for Ce-bearing alkali borate glasses. When plotting the log $[Ce^{4+}/Ce^{3+}]$ vs. reciprocal temperature the authors observed the expected linear correlation, but interestingly they observed that the slope of the straight lines (considered proportional to the thermodynamic standard enthalpy of reduction[3]) was increasing as the glass basicity increased (from 0.16 for Li up to 0.4 for K-glasses).

Schreiber and coauthors (Schreiber, 1980; Schreiber et al., 1994; Schreiber et al., 1980) described the Ce^{4+}-Ce^{3+} equilibria in glasses with respect to bulk chemistry, temperature, oxygen fugacity conditions, and Ce amount (from 0.5 to 1.3wt%). The authors reported that the dependence of the Ce equilibria with respect to the -log (fO_2) to be ~4, in Ca-Mg aluminosilicate glasses. However, contrary to Paul and Douglas (1965a), Schreiber and coauthors observed no dependence of Ce redox ratio on the Ce concentration.

Baucke and Duffy (1993) considered existing redox equilibria in alkali silicate melts (at 1400 °C, in air) and report their correlation with the optical basicity Λ of the melt for several multivalent elements. The authors stated that it is possible to predict the redox equilibria from the composition. By plotting the log $[Ce^{3+}/Ce^{4+}]$ against optical basicity values, they determined a relationship from the straight line obtained, suggesting that it would be feasible to express the ratio of ionic concentrations merely in terms of the optical basicity (Baucke & Duffy, 1993). For Ce equilibrium, the authors proposed the following relationship:

$$\log\left[Ce^{3+}/Ce^{4+}\right] = 5.4 - 8.3\Lambda, \qquad (19.6)$$

More recently, Pinet et al. (2006) proposed a model relating the Ce redox ratio to oxygen fugacity, temperature, and optical basicity in silicate glasses (suitable for nuclear waste management). Moreover, the authors report that cerium solubility is strongly affected by redox state, and that Ce solubility is improved when incorporated in the reduced Ce^{3+} form. Pinet and coauthors (2006) developed a general model (similar to the one used for iron in the well-known Kress and Carmichael model; Kress & Carmichael, 1991) applicable to various silicate glass compositions (optical basicity values from 0.52 to 0.65) and temperatures in the range ~900–1240 °C.

A few recent studies have been carried out, aiming to understand the evolution of cerium redox state on temperature, pressure, and bulk composition, by using XAS (Burnham & Berry, 2014; Smythe & Brenan, 2015, 2016; Smythe et al., 2013). Interestingly, these studies report contradictory findings regarding the dependence of the $[Ce^{3+}/Ce^{4+}]$ redox ratio on melt/glass polymerization. Indeed, Burnham and Berry's (2014) results corroborate findings from previous studies (Schreiber et al., 1980; Baucke & Duffy, 1993; Pinet et al., 2006), indicating that the content of reduced species increases with increasing melt polymerization or temperature. On the contrary, Smythe et al. (2013, 2015) observed that the abundance of Ce^{4+} decreases with decreasing polymerization.

Smythe and coauthors (2013, 2015) studied anhydrous alkali-aluminosilicate glasses (synthetic basalt, andesite, dacite, and rhyolite glasses; all sets include alkali and TiO_2, and are Fe-free) that contained ~1.0 wt% CeO_2. Other sets of hydrous glasses were prepared at 0.001GPa and 1GPa to assess the effect of water (hydrous compositions favour the stabilization of reduced species). $[Ce^{3+}/Ce^{4+}]$ redox ratio assessment was carried out both by potentiometric titration and XAS ($M_{4,5}$-edges). Burnham and Berry (2014) studied the influence of bulk composition on the oxidation state of cerium, for a larger range of oxygen fugacity values (from FMQ-10 to FMQ+11) in alkali-free and Fe-free aluminosilicate compositions (the same diopside-anorthite compositions described above for Eu) doped with ~0.5 wt% CeO_2. Both authors report the possible occurrence of Ce redox modifications under the beam during XAS measurements.

From the available data, Smythe and Brenan (2015) ascribed the contrasting effect of glass composition on Ce redox ratio to the compositional differences. In the studies from Smythe and coauthors (2013, 2015) the four compositions span from basaltic to granitic, covering wide ranges of SiO_2 contents (from ~52 to ~78 mol% SiO_2) and (Si+Al)/alkali molar ratios (Smythe et al., 2013; Smythe & Brenan, 2015). Nevertheless, only a

[3] ΔH^0, generally speaking, represents the energy required for the reduction reaction.

limited dataset is reported. On the other hand, Burnham and Berry (2014) studied a much larger dataset (11 different compositions), and a wider range of oxygen fugacity conditions tested. However, all glasses in the diopside-anorthite system have SiO_2 < 65 mol%, extremely high amounts of (CaO+MgO), and no alkalies. Another point that could be source of the differences between the studies lies in the experimental technique employed for the estimation of the Ce^{3+}/Ce^{4+} redox ratio. Both authors used XAS spectroscopy even if at different edges (hence, by looking at different electronic transitions). Smythe et al. (2013) reported beam-damage and overestimation of the Ce^{4+} compared to wet chemistry analyses, thus proposing an empirical relation for correction of the Ce^{3+}/Ce^{4+} redox ratios, based on the potentiometric data. Burnham and Berry (2014) asserted that beam-induced changes were observed only for samples prepared at high pressures. The combination of XAS techniques with other analytical methods could have provided more insights on the effect of the X-ray beam on Ce redox ratio, however the authors did not report any further investigation. For example, optical absorption (OA) and photoluminescence (PL) measurements or XPS analysis, before and after the beam exposure, would have been useful to understand to what extent the X-ray beam influenced cerium ions.

More recently, Cicconi et al. (2017, 2020, 2021) investigated cerium speciation in alkali-silicate and aluminosilicate glasses and Ce-activated optical silica fibers. The authors also used XAS to quantify the Ce redox ratio, but also combined Raman and optical spectroscopy (PL) techniques. Cicconi and coauthors (2017), in agreement with Burnham and Berry (2014) and other previous studies observed that Ce redox behavior, in Na-silicate and aluminosilicate glasses, is linked to the optical basicity of the glasses, and the substitution of Al for Na strongly stabilizes reduced Ce species. However, for optical silica fibers Ce/Al codoped, the relationship bulk chemistry/redox was found to be more complex. In fact, in these glasses, the theoretical optical basicity parameter cannot be used anymore to predict the Ce redox changes, because the different Al structural role (coordinations) in the silica fibers network induces modifications in the Ce^{3+} structural environment that the optical basicity concept cannot predict (variations of the distance between Ce^{3+} and its ligands, a/o variations of the <Ce-O> bonds covalency). Thus, Ce redox state is critically affected by the nature of the cations present in the silica glass network (Cicconi et al., 2017, 2021). Raman spectroscopy analyses of Ce-bearing sodium-silicate and aluminosilicate glasses highlight the structural variations occurring when cerium is stabilized with different valences in the glass network. These observation reported by Cicconi et al. (2017) could explain the contradictory results of Smythe and coauthors

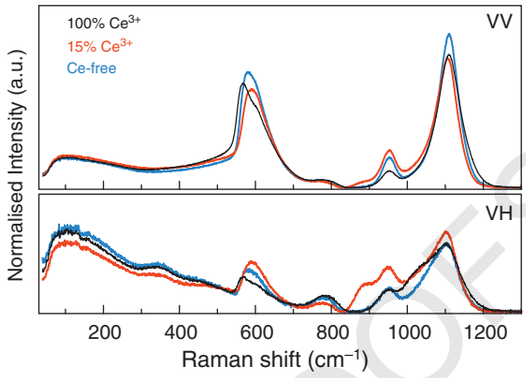

Figure 19.7 Parallel (VV) and cross-polarized (VH) Raman spectra (normalized to the total area) for a NS2 glass (blue line), and for Ce doped glasses. Black lines refer to a NS2 glass having 100%Ce^{3+} ions, and red lines to the glass with 15% Ce^{3+} ions (error on redox quantification: ±7; data from Cicconi et al., 2021).

(Smythe et al., 2013; Smythe & Brenan, 2015) and emphasize the need for understanding an element structural role, rather than limiting studies to redox changes.

Raman spectroscopy is a powerful, complementary technique that may be used in order to understand the ion structural behavior. Parallel (VV) and cross-polarized (VH) Raman spectra for Ce-free and Ce-bearing sodium-disilicate glasses (NS2) are reported in Figure 19.7 (from Cicconi et al., 2021). Silica vibrations related either to Si-O-Si ring motions or Si-O stretching motions are highly polarized bands (Hehlen & Neuville, 2015), thus their intensity drastically decreases when collected as cross-polarized (factor 1:9 in Figure 19.7). For example, the bands in the high frequency portion of the Raman spectra (~800–1300cm^{-1}), related to symmetric stretching, significantly change their intensity, though without changing the frequency position. The VV and VH spectra for the glass containing only reduced species (100±7% Ce^{3+}: black lines in Figure 19.7) indicate a higher polymerization of the network, additionally confirmed by the increase of the glass transition temperature (Cicconi et al., 2021). On the contrary, the prevalent presence of oxidized species (15±7% Ce^{3+}: red lines in Figure 19.7) induces an increase of Q^2 and Q^3 species[4], and the appearance of an additional band around 880 cm^{-1}, which is polarized (indication a non-symmetric vibration). From the available data the authors concluded that, depending on the Ce^{3+}/Ce^{4+} redox ratio, strong variations occur in the silica glass network, arising from Ce-NBO(BO) interactions.

[4] Q^n species: Q represents a Si centred tetrahedron and n the number of bridging oxygen atoms (n= 0 – 4).

Optical spectroscopy is widely used to investigate REE- and transition element-bearing glasses, because of the extremely high sensitivity, and because these techniques are able to detect small variations in the surrounding ligand (e.g., variations of the covalency). OA and PL spectroscopies have been extensively used to study Ce-doped materials (e.g., Assefa et al., 2004; Brandily-Anne et al., 2010; Fasoli et al., 2009; Herrmann et al., 2015), even if the quantification of Ce redox state is very controversial. As a matter of fact, Ce species present absorption in the UV-region with an overlap of the broad bands, which increase or decrease depending on glass chemistry, and Ce content. Moreover, only Ce^{3+} is optically active and has fluorescence emission, whereas Ce^{4+} does not show luminescence due to its closed electronic shell ([Xe] $4f^0$).

A combination of wet-chemistry, voltammetry, Raman, and XAS with optical techniques could provide a better understanding of the factors influencing the Ce redox ratio and speciation, in silicate glasses and melts.

19.3.3. Influence of Other Elements: Mutual Interactions

In the glass industry, controlling the color of the final product is a very important issue along with the fining process (the removal of gaseous inclusions). Hence, several investigations in glass and ceramic manufacturing involve understanding the effect of multivalent elements on the final color (as well as on properties). REE have been widely used in the production of special glasses, or as decolorizing agents (Ce). For example, in common window glasses (soda-lime-silica) production, the presence of divalent iron is unwanted because of a strong blue hue, and Ce_2O_3 is considered a particularly effective oxidizing agent. Glass with iron impurities up to 0.1wt% might be successfully decolorized by adding sulfates (as fining agent) and cerium oxide (Henderson, 1984).

In the past, cerium has been used in the production of special glasses for protection against UV light. Indeed, earlier studies on the ceria/ceric equilibria were done on simple binary systems in order to determine the effect of composition on cerium absorption bands and, in turn, on the UV cut-off (Paul et al., 1976). More recently, the interest for REE redox control derives from the use of glasses as nuclear waste immobilizer. For this purpose, the parameters influencing cerium redox state have been studied in many silicate and borate compositions (Pinet et al., 2014; Pinet et al., 2006). Lanthanides have properties similar to the transuranic actinides, so REE have been considered as actinide analogues for preliminary modelling of the characteristics of the waste forms. Indeed, REE are the most favored elements to be used as surrogates since they already occur as fission products; moreover, because of the geochemical similarity with actinides, they provide a way to forecast the long-term behavior of waste forms.

Another important point in glass/ceramic manufacturing concerns the understanding of the mutual interactions between multivalent elements in glasses. Both Ce and Eu redox ratios are influenced by the presence of other multivalent elements, as described by (Schreiber et al. (1987). A complete understanding of such interactions between transition elements and REE is as important for glass manufacturing, as it is for geochemical and petrological interpretations of element partitioning between melt and crystals.

The use of Ce_2O_3 as decolorizing agent implies that an interaction between different multivalent elements occurs, following the reaction (Schreiber et al. 1987):

$$Fe^{2+}_{melt} + Ce^{4+}_{melt} = Fe^{3+}_{melt} + Ce^{3+}_{melt}, \qquad (19.7)$$

The interaction between redox species has been argued to derive either from electron exchanges at high temperatures (melts as analogs of aqueous solution) or exclusively during the quench, implying a charge transfer process due to presence of Ce-O-Fe complexes. Unfortunately, the study of mutual interaction and of the redox behavior in melts has been limited to relatively few systems because of the experimental difficulties related with the measurements.

19.3.3.1. Fe-Eu Mutual Interactions. Since iron is the most common transition element in natural magmas, it provides a first order control on properties (see Le Losq et al., 2021, Chapter 12, this volume, for details), and since it is present in amounts orders of magnitude higher than REE (or other transition elements), it also buffers the magma redox state.

Most of the studies described in this chapter refer to Fe-free glasses and only a few report data for Fe-bearing glasses and discuss the possible differences. Schreiber and coauthors, in their studies, attempted to understand the redox reactions not only in iron-free compositions, but also in more realistic systems in order to develop models applicable to natural magmas (e.g., Schreiber, 1980; Schreiber et al., 1982; Schreiber et al., 1980, 1987). A chemical equation for the interaction by oxidation-reduction of Eu and Fe ions in silicate melts, similar to Equation 19.7, could be expressed as:

$$Fe^{3+}_{melt} + Eu^{2+}_{melt} = Fe^{2+}_{melt} + Eu^{3+}_{melt}, \qquad (19.8)$$

The occurrence of this interaction in glasses has been experimentally verified both for Eu-bearing simplified systems (CMAS, Na-silicate, DiAn) and multicomponent ones (basalts). The presence of both multivalent elements determines different redox kinetics, and the stabilization of higher amounts of reduced iron species (Schreiber et al., 1980, 1982; Cicconi, 2010; Cicconi et al., 2015).

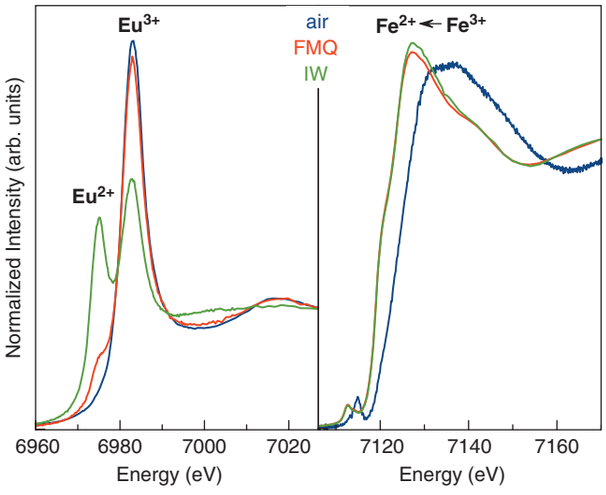

Figure 19.8 X-Ray Absorption Spectroscopy data at the Eu L_{III}-edge (left) and at the Fe K-edge (right) for glasses of Di-An composition synthetized under different conditions of fO_2 (data from Cicconi et al., 2017).

For example, XAS data collected for a series of DiAn glass compositions (with Eu/Fe molar ratio = 0.05) show that, for both species, the evolution of the redox ratios with fO_2 changes with respect to the glasses containing only a single multivalent element. Indeed, Fe-doped DiAn glasses prepared at ambient conditions (1400 °C, in air) should have trivalent iron as the predominant species. However, the presence of europium (Figure 19.8), leads to the stabilization of > 30% Fe^{2+} in air (±5; Cicconi, 2010). Moreover, at oxygen fugacity values close to the FMQ buffer, Fe is already almost completely reduced (> 90% Fe^{2+}±5) and the Eu^{2+}/Eu^{3+} redox ratio is lower than expected (~5% Eu^{2+}±6). On the contrary, close to the IW buffer, when all iron is completely reduced, the $Eu^{2+}/(Eu^{2+} + Eu^{3+})$ estimated for the Fe/Eu glass is 0.49 (±0.06), very close to the one estimated for the Fe-free glass (0.47±0.06). Thus, it is reasonable to consider that europium redox equilibrium goes back to the expected value when all trivalent iron disappears from the melt.

From the data reported in Figure 19.5 it is possible to observe that for oxygen fugacity values close to the FMQ buffer (-log(fO_2) ~6 in Figure 19.5) the Eu redox ratio in Fe-free glasses is highly variable depending on the bulk chemistry. However, the introduction of iron into the system strongly decreases this variability.

As previously reported, two mechanisms could be responsible for the lower Eu^{2+} contents: electron exchanges in the melt, or the occurrence of oxidation via charge transfer processes during glass quenching. In order to monitor the possible mutual interaction at high temperatures (and avoid possible quenching effects), a study of molten materials where both Fe and Eu redox kinetics were simultaneously monitored under imposed oxygen fugacity conditions was carried out by Cicconi et al. (2015). The studied composition was a Fe-rich basalt containing ~5 wt% Eu_2O_3 (to obtain an Eu/Fe molar ratio = 0.066).

Some of the in-situ dispersive X-ray Absorption Spectroscopy data, obtained at high temperatures (HT=1500 °C) for a basaltic glass are reported in Figure 19.9a, and the resulting redox kinetics for both Eu and Fe are shown in Figure 19.9b. At HT, both in air and under pure Ar, the stabilization of small amount of divalent europium would be expected. However, the presence of iron hampers any Eu reduction. Only under more reducing conditions (Ar/H_2), and after almost complete reduction of all iron present, do Eu ions start to be stabilized as Eu^{2+} (Figs. 19.9a,b). From the in-situ study, Cicconi et al. (2015) affirm that there is strong competition between the two redox couples in the melt, implying that electron exchange occurs also in the molten material. Moreover, they observed differences in the Eu redox ratio from the melt and the in-situ quenched glass, emphasizing that the quench effect must not be neglected in future studies of Eu/Fe-bearing glasses.

19.3.4. Other Multivalent Rare Earth Elements

As stated above, in geological systems (aqueous solution, glass, and rocks) the most stable valence for lanthanides is the trivalent one. However, REE can be stabilized with other oxidation states. In the past decades REE-bearing glass, glass-ceramic, or crystalline materials have been developed for the characteristic luminescence properties provided by the lanthanides (Lucas et al., 2014). Based on these studies, several other lanthanides have been observed to be stable as divalent or tetravalent.

• divalent REE: Eu^{2+}. Sm^{2+}, Yb^{2+}

Eu is able to lose two electrons in order to obtain the stabilization of the half-full *4f* shell: Eu^{2+} [Xe]$4f^7$, and similar considerations can be done for Sm (Sm^{2+} [Xe] $4f^6$). Yb^{2+} can be formed due to the stabilization of the full *4f* shell [Xe]$4f^{14}$.

The stabilization of divalent REE ions in different host materials has been realized either by using a highly reducing atmosphere (H_2), by electrolytic reduction, or by exposing the material to ionizing radiation (Fong, 1964; Nicoara et al., 2008; Nogami et al., 1995).

• Tetravalent REE: Ce^{4+}, Pr^{4+}, Tb^{4+}

The known forms, obtained under oxidizing conditions, are:

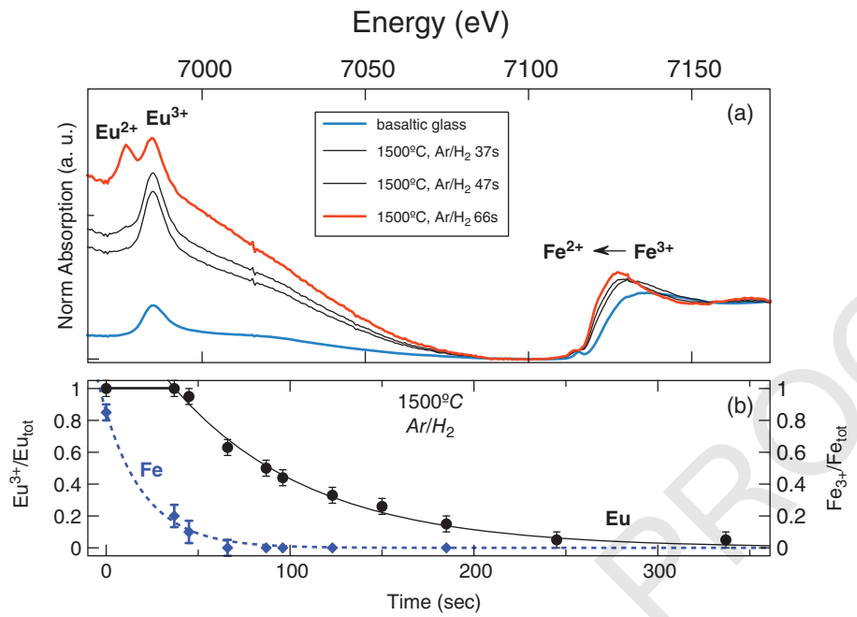

Figure 19.9 (a) XAS spectra, normalized at the Fe K-edge, collected for the starting basaltic glass and for the melt (1500°C), after 37, 47 and 66s under reducing conditions (Ar/H_2 gas). (b) Time dependence of Eu and Fe redox kinetics in the basaltic melt, under reducing conditions (data from Cicconi et al., 2015).

Ce, which lose all four outer electrons to form Ce^{4+} ions $[Xe]4f^0$. Similarly Pr^{4+} and Tb^{4+} can be formed (Morgan et al., 1987; Ueda et al., 2017).

19.4. CONCLUSIONS AND PERSPECTIVES

Trace element geochemistry gives important information in Earth and planetary sciences for investigating problems ranging from geochemistry to igneous petrology (crystal-melt equilibria, magmatic differentiation, etc.). REE distributions in minerals are strongly dependent on (i) ionic radius, and (ii) the suitable valence state and bonding forces (as in the case of monazite and xenotime) and the lack of constraints regarding element partition coefficients is a major source of error in modelling crystal/melt fractionation (Blundy & Wood, 2003, and references therein).

Many geologically important trace elements are potentially redox variable (e.g., Ti, V, Cr, Cu, Eu, Ce), however the factors influencing redox mechanisms sometimes are poorly known, thus limiting our understanding of trace element patterns, abundances, and partitioning. Determining an element oxidation state, coordination environment, and speciation provide the basic knowledge on the parameters controlling the element geochemical behavior.

The data reported here emphasize the need for understanding the redox behavior in many other systems, but also emphasize the importance of an often-underestimated parameter: the elements' structural role. There are only a few examples, in the Earth Sciences literature, where systematic studies of Ce and Eu redox are complemented with data regarding their surroundings. The combination of advanced element specific techniques (such as XAS) with other analytical methods might provide more insights on the effect of the element speciation in glasses and melts.

ACKNOWLEDGMENTS

Some of the data here shown have been acquired at LISA and at ODE beamlines, and we acknowledge ESRF (France) and SOLEIL (France) for provision of synchrotron radiation facilities.

REFERENCES

Assefa, Z., Haire, R. G., Caulder, D. L., & Shuh, D. K. (2004). Correlation of the oxidation state of cerium in sol--gel glasses as a function of thermal treatment via optical spectroscopy and XANES studies. *Spectrochimica Acta Part A: Molecular and Biomolecular Spectroscopy*, *60*, 8, 1873–1881. https://doi.org/10.1016/j.saa.2003.10.005

Ballard, J. R., Palin, M. J., & Campbell, I. H. (2002). Relative oxidation states of magmas inferred from Ce(IV)/Ce(III) in zircon: application to porphyry copper deposits of northern

Chile. *Contributions to Mineralogy and Petrology*, *144*, 3, 347–364. https://doi.org/10.1007/s00410-002-0402-5

Baucke, F., & Duffy, J. (1993). Redox reactions between cations of different polyvalent elements in glass melts: an optical basicity study. *Physics and Chemistry of Glasses*

Bédard, J. H. (2006). Trace element partitioning in plagioclase feldspar. *Geochimica et Cosmochimica Acta*, *70*, 14, 3717–3742. https://doi.org/10.1016/J.GCA.2006.05.003

Blundy, J., & Wood, B. (2003). Partitioning of trace elements between crystals and melts. *Earth and Planetary Science Letters*, *210*, 3–4, 383–397. https://doi.org/10.1016/S0012-821X(03)00129-8

Brandily-Anne, M. L., Lumeau, J., Glebova, L., & Glebov, L. B. (2010). Specific absorption spectra of cerium in multicomponent silicate glasses. In *Journal of Non-Crystalline Solids*, *356*, 2337–2343). https://doi.org/10.1016/j.jnoncrysol.2010.02.020

Brugger, J., Etschmann, B., Chu, Y. S., Harland, C., Vogt, S., Ryan, C., & Jones, H. (2006). The oxidation state of europium in hydrothermal scheelite: In situ measurement by XANES spectroscopy. *Canadian Mineralogist*, *44*, 5, 1079–1087. https://doi.org/10.2113/gscanmin.44.5.1079

Burnham, A. D., Berry, A. J., Halse, H. R., Schofield, P. F., Cibin, G., & Mosselmans, J. F. W. (2015). The oxidation state of europium in silicate melts as a function of oxygen fugacity, composition and temperature. *Chemical Geology*, *411*, 248–259. https://doi.org/10.1016/j.chemgeo.2015.07.002

Burnham, A. D., & Berry, A. J. (2014). The effect of oxygen fugacity, melt composition, temperature and pressure on the oxidation state of cerium in silicate melts. *Chemical Geology*, *366*, 52–60. https://doi.org/10.1016/j.chemgeo.2013.12.015

Ching-oh, S., Williams, R. J., & Shine-soon, S. (1974). Distribution coefficients of Eu and Sr for plagioclase-liquid and clinopyroxene-liquid equilibria in oceanic ridge basalt: an experimental study. *Geochimica et Cosmochimica Acta*, *38*, 9, 1415–1433. https://doi.org/10.1016/0016-7037(74)90096-9

Cicconi, M. R., Neuville, D. R., Blanc, W., Lupi, J.-F., Vermillac, M., & de Ligny, D. (2017). Cerium/aluminum correlation in aluminosilicate glasses and optical silica fiber preforms. *Journal of Non-Crystalline Solids*, *475*, 85–95. https://doi.org/10.1016/j.jnoncrysol.2017.08.035

Cicconi, M. R., Blanc, W., de Ligny, D., & Neuville, D. R. (2020). The influence of codoping on optical properties and glass connectivity of silica fiber preforms. *Ceramics International*, *46*, 26231–26259. https://doi.org/10.1016/j.ceramint.2020.05.233

Cicconi, M. R., Veber, A., Neuville, D. R., Baudelet, F., & de Ligny, D. (2021). Cerium speciation in silicate glasses: Structure-property relationships. *Journal of Non-Crystalline Solids.*

Cicconi, M. R. (2010). *Europium (Eu) and cerium (Ce) in silicate glasses: XAS study of their oxidation states and local environments*. PhD thesis, Camerino University.

Cicconi, M. R., Giuli, G., Paris, E., Ertel-Ingrisch, W., Ulmer, P., & Dingwell, D. B. B. (2012). Europium oxidation state and local structure in silicate glasses. *American Mineralogist*, *97*, 5–6, 918–929. https://doi.org/10.2138/am.2012.4041

Cicconi, M. R., Neuville, D. R., Tannou, I., Baudelet, F., Floury, P., Paris, E., & Giuli, G. (2015). Competition between two redox states in silicate melts: An in-situ experiment at the Fe K-edge and Eu L<inf>3</inf>-edge. *American Mineralogist*, *100*, 4, 1013–1016. https://doi.org/10.2138/am-2015-5172

Cicconi, M. R., Veber, A., de Ligny, D., Rocherullé, J., Lebullenger, R., & Tessier, F. (2017). Chemical tunability of europium emission in phosphate glasses. *Journal of Luminescence*, *183*. https://doi.org/10.1016/j.jlumin.2016.11.019

Cicconi, M. R., Giuli, G., Ertel-Ingrisch, W., Paris, E., & Dingwell, D. B. (2015). The effect of the [Na/(Na+K)] ratio on Fe speciation in phonolitic glasses. *American Mineralogist*, *100*, 7, 1610–1619. https://doi.org/10.2138/am-2015-5155

Colson, R. O., Haskin, L. A., & Crane, D. (1990). Electrochemistry of cations in diopsidic melt: Determining diffusion rates and redox potentials from voltammetric curves. *Geochimica et Cosmochimica Acta*, *54*, 12, 3353–3367. https://doi.org/10.1016/0016-7037(90)90290-2

Concas, G., Congiu, F., Spano, G., Speghini, A., & Gatterer, K. (1998). Mössbauer investigation of rare earth sites in europium containing glasses. *Journal of Non-Crystalline Solids*, *232–234*, 341–345. https://doi.org/10.1016/S0022-3093(98)00390-1

Dietzel, A. (1948). Glasstruktur und Glaseigenschaften. *Glastechnische Berichte*, *22*, 41–50.

Drake, M. J. (1975). The oxidation state of europium as an indicator of oxygen fugacity. *Geochimica et Cosmochimica Acta*, *39*, 1, 55–64. https://doi.org/10.1016/0016-7037(75)90184-2

Drake, M. J., & Weill, D. F. (1975). Partition of Sr, Ba, Ca, Y, Eu^{2+}, Eu^{3+}, and other REE between plagioclase feldspar and magmatic liquid: an experimental study. *Geochimica et Cosmochimica Acta*, *39*, 5, 689–712. https://doi.org/10.1016/0016-7037(75)90011-3

Duffy, J. A., & Ingram, M. D. (1971). Establishment of an optical scale for Lewis basicity in inorganic oxyacids, molten salts, and glasses. *Journal of the American Chemical Society*, *93*, 24, 6448–6454. https://doi.org/10.1021/ja00753a019

Duffy, J. A., & Ingram, M. D. (1976). An interpretation of glass chemistry in terms of the optical basicity concept. *Journal of Non-Crystalline Solids*, *21*, 3, 373–410. https://doi.org/10.1016/0022-3093(76)90027-2

Duffy, John A. (1993). A review of optical basicity and its applications to oxidic systems. *Geochimica et Cosmochimica Acta*, *57*, 16, 3961–3970. https://doi.org/10.1016/0016-7037(93)90346-X

Elderfield, H., & Greaves, M. J. (1981). Negative cerium anomalies in the rare earth element patterns of oceanic ferromanganese nodules. *Earth and Planetary Science Letters*, *55*, 1, 163–170. https://doi.org/10.1016/0012-821X(81)90095-9

Evensen, N. M., Hamilton, P. J., & O'Nions, R. K. (1978). Rare-earth abundances in chondritic meteorites. *Geochimica et Cosmochimica Acta*, *42*, 8, 1199–1212. https://doi.org/10.1016/0016-7037(78)90114-X

Fasoli, M., Vedda, A., Lauria, A., Moretti, F., Rizzelli, E., Chiodini, N., et al. (2009). Effect of reducing sintering atmosphere on Ce-doped sol-gel silica glasses. *Journal of Non-Crystalline Solids*, *355*, 18–21, 1140–1144. https://doi.org/10.1016/j.jnoncrysol.2009.01.043

Fong, F. K. (1964). Electrolytic Reduction of Trivalent Rare-Earth Ions in Alkaline-Earth Halides. *The Journal of*

Chemical Physics, *41*, 8, 2291–2296. https://doi.org/10.1063/1.1726262

Fraser, D. G. (1975). Activities of trace elements in silicate melts. *Geochimica et Cosmochimica Acta*, *39*, 11, 1525–1530. https://doi.org/10.1016/0016-7037(75)90154-4

Gaetani, G. A., & Grove, T. L. (1995). Partitioning of rare earth elements between clinopyroxene and silicate melt Crystal-chemical controls. *Geochimica et Cosmochimica Acta*, *59*, 10, 1951–1962. https://doi.org/10.1016/0016-7037(95)00119-0

Gaft, M., Reisfeld, R., & Panczer, G. G. (2015). *Modern Luminescence Spectroscopy of Minerals and Materials*. Cham: Springer International Publishing. https://doi.org/10.1007/978-3-319-24765-6

Grutzeck, M., Kridelbaugh, S., & Weill, D. (1974). The distribution of Sr and REE between diopside and silicate liquid. *Geophysical Research Letters*, *1*, 6, 273–275. https://doi.org/10.1029/GL001i006p00273

Harmening, T., Hermes, W., Eul, M., & Pöttgen, R. (2010). Mixed valent stannide EuRuSn3 – Structure, magnetic properties, and Mössbauer spectroscopic investigation. *Solid State Sciences*, *12*, 2, 284–290. https://doi.org/10.1016/J.SOLIDSTATESCIENCES.2009.11.009

Hehlen, B., & Neuville, D. R. (2015). Raman response of network modifier cations in alumino-silicate glasses. *Journal of Physical Chemistry B*, *119*, 10, 4093–4098. https://doi.org/10.1021/jp5116299

Henderson, P. (1984). *Rare earth element geochemistry*. Elsevier.

Herrmann, A., Othman, H. A., Assadi, A. A., Tiegel, M., Kuhn, S., & Rüssel, C. (2015). Spectroscopic properties of cerium-doped aluminosilicate glasses. *Optical Materials Express*, *5*, 4, 720. https://doi.org/10.1364/OME.5.000720

Johnston, W. D. (1964). Oxidation-Reduction Equilibria in Iron-Containing Glass. *Journal of the American Ceramic Society*, *47*, 4, 198–201. https://doi.org/10.1111/j.1151-2916.1964.tb14392.x

Johnston, W. D. (1965). Oxidation-Reduction Equilibria in Molten Na2O.2SiO2 Glass. *Journal of the American Ceramic Society*, *48*(4), 184–190. https://doi.org/10.1111/j.1151-2916.1965.tb14709.x

Karner, J. M., Papike, J. J., Sutton, S. R., Burger, P. V., Shearer, C. K., Le, L., et al. (2010). Partitioning of Eu between augite and a highly spiked martian basalt composition as a function of oxygen fugacity (IW-1 to QFM): Determination of Eu2+/Eu3+ ratios by XANES. *American Mineralogist*, *95*, 2–3, 410–413. https://doi.org/10.2138/am.2010.3394

Kress, V. C., & Carmichael, I. S. E. (1991). The compressibility of silicate liquids containing Fe2O3 and the effect of composition, temperature, oxygen fugacity and pressure on their redox states. *Contributions to Mineralogy and Petrology*, *108*, 1–2, 82–92. https://doi.org/10.1007/BF00307328

Lauer, H. V., & Morris, R. V. (1977). Redox Equilibria of Multivalent Ions in Silicate Glasses. *Journal of the American Ceramic Society*, *60*, 9–10, 443–451. https://doi.org/10.1111/j.1151-2916.1977.tb15530.x

Lebouteiller, A., & Courtine, P. (1998). Improvement of a bulk optical basicity table for oxidic systems. *Journal of Solid State Chemistry*, *137*, 94–103. https://doi.org/10.1006/jssc.1997.7722

Le Losq, C., Cicconi, M. R., & Neuville, D. R. (2021). Iron in silicate glasses and melts: Implications for volcanological processes. In Moretti, R., & Neuville, D. R. (Eds.), *Redox Magma Geochemistry*. Geophysical Monograph Series 266. American Geophysical Union.

Lipin, B. R., & McKay, G. A. (1989). *Geochemistry and mineralogy of rare earth elements*. Mineralogical Society of America.

Lucas, J., Lucas, P., Le Mercier, T., Rollat, A., & Davenport, W. G. (2014). *Rare earths: science, technology, production and use*. Elsevier.

Masuda, A., Tanaka, T., Nakamura, N., & Kurasawa, H. (1974). Possible REE anomalies of Apollo 17 REE patterns. In: *Lunar Science Conference, 5th, Houston, Tex., March 18-22, 1974, Proceedings. Volume 2. (A75-39540 19-91)* New York, Pergamon Press, Inc., 1974, pp. 1247–1253.

McIntire, W. L. (1963). Trace element partition coefficients—a review of theory and applications to geology. *Geochimica et Cosmochimica Acta*, *27*, 12, 1209–1264. https://doi.org/10.1016/0016-7037(63)90049-8

McKay, G. A. (1989). Partitioning of rare earth elements between major silicate minerals and basaltic melts. In *Reviews in Mineralogy and Geochemistry*, *21*, 45–77.

Moretti, R. (2005). Polymerisation, basicity, oxidation state and their role in ionic modelling of silicate melts. *Annals of Geophysics*, *48*, 4/5, 583–608.

Moretti, R., & Ottonello, G. (2003). Polymerization and disproportionation of iron and sulfur in silicate melts: Insights from an optical basicity-based approach. In *Journal of Non-Crystalline Solids*, *323*, 111–119. https://doi.org/10.1016/S0022-3093(03)00297-7

Morgan, S. H., Magruder, R. H., & Silberman, E. (1987). Raman Spectra of Rare-Earth Phosphate Glasses. *Journal of the American Ceramic Society*, *70*, 12, C-378-C–380. https://doi.org/10.1111/j.1151-2916.1987.tb04925.x

Morris, R., & Haskin, L. (1974). EPR measurement of the effect of glass composition on the oxidation states of europium. *Geochimica et Cosmochimica Acta*, *38*, 9, 1435–1445. https://doi.org/10.1016/0016-7037(74)90097-0

Morris, R., Haskin, L., Biggar, G., & O'Hara, M. (1974). Measurement of the effects of temperature and partial pressure of oxygen on the oxidation states of europium in silicate glasses. *Geochimica et Cosmochimica Acta*, *38*, 9, 1447–1459. https://doi.org/10.1016/0016-7037(74)90098-2

Müller, P., & Muecke, G. K. (1984). Significance of Europium anomalies in silicate melts and crystal-melt equilibria: a re-evaluation. *Contributions to Mineralogy and Petrology*, *87*, 3, 242–250. https://doi.org/10.1007/BF00373057

Nicoara, I., Pecingina-Garjoaba, N., & Bunoiu, O. (2008). Concentration distribution of Yb2+ and Yb3+ ions in YbF3: CaF2 crystals. *Journal of Crystal Growth*, *310*, 7–9, 1476–1481. https://doi.org/10.1016/J.JCRYSGRO.2007.11.024

Nogami, M., Abe, Y., Hirao, K., & Cho, D. H. (1995). Room temperature persistent spectra hole burning in Sm2+-doped silicate glasses prepared by the sol-gel process. *Applied Physics Letters*, *66*, 22, 2952–2954. https://doi.org/10.1063/1.114240

O'Hara, M. J. (1995). Trace Element Geochemical Effects of Integrated Melt Extraction and "Shaped" Melting Regimes.

Journal of Petrology, *36*, 4, 1111–1132. https://doi.org/10.1093/petrology/36.4.1111

Onuma, N., Higuchi, H., Wakita, H., & Nagasawa, H. (1968). Trace element partition between two pyroxenes and the host lava. *Earth and Planetary Science Letters*, *5*, 47–51. https://doi.org/10.1016/S0012-821X(68)80010-X

Ottonello, G., Moretti, R., Marini, L., & Vetuschi Zuccolini, M. (2001). Oxidation state of iron in silicate glasses and melts: A thermochemical model. *Chemical Geology*, *174*, 1–3, 157–179. https://doi.org/10.1016/S0009-2541(00)00314-4

Papike, J. J., Karner, J. M. M., & Shearer, C. K. K. (2005). Comparative planetary mineralogy: Valence state partitioning of Cr, Fe, Ti, and V among crystallographic sites in olivine, pyroxene, and spinel from planetary basalts. *American Mineralogist*, *90*, 2–3, 277–290. https://doi.org/10.2138/am.2005.1779

Paul, A., & Douglas, R. W. (1965a). Cerous-ceric equilibrium in binary alkali borate and alkali silicate glasses. *Physics and Chemistry of Glasses*, *6*, 6, 212–215.

Paul, A., & Douglas, R. W. (1965b). Ferrous-ferric equilibrium in binary alkali silicate glasses. *Physics and Chemistry of Glasses*, *6*, 6, 207–211.

Paul, A., Mulholland, M., & Zaman, M. S. (1976). Ultraviolet absorption of cerium(III) and cerium(IV) in some simple glasses. *Journal of Materials Science*, *11*, 11, 2082–2086. https://doi.org/10.1007/PL00020336

Philpotts, J. A. (1970). Redox estimation from a calculation of Eu2+ and Eu3+ concentrations in natural phases. *Earth and Planetary Science Letters*, *9*, 3, 257–268. https://doi.org/10.1016/0012-821X(70)90036-1

Pinet, O., Hugon, I., & Mure, S. (2014). Redox Control of Nuclear Glass. *Procedia Materials Science*, *7*, 124–130. https://doi.org/10.1016/J.MSPRO.2014.10.017

Pinet, O., Phalippou, J., & Di Nardo, C. (2006). Modeling the redox equilibrium of the Ce4+/Ce3+ couple in silicate glass by voltammetry. *Journal of Non-Crystalline Solids*, *352*, 50–51, 5382–5390. https://doi.org/10.1016/j.jnoncrysol.2006.08.034

Rakovan, J., Newville, M., & Sutton, S. (2001). Evidence of heterovalent europium in zoned llallgua apatite using wavelength dispersive XANES. *American Mineralogist*, *86*, 5–6, 697–700. https://doi.org/10.2138/am-2001-5-610

Rollinson, H. R. (1993). *Using geochemical data : evaluation, presentation, interpretation*. Longman Scientific & Technical.

Schnetzler, C., & Philpotts, J. A. (1970). Partition coefficients of rare-earth elements between igneous matrix material and rock-forming mineral phenocrysts—II. *Geochimica et Cosmochimica Acta*, *34*, 3, 331–340. https://doi.org/10.1016/0016-7037(70)90110-9

Schreiber, H. D. (1980). Properties of redox ions in glasses: An interdisciplinary perspective. *Journal of Non-Crystalline Solids*, *42*, 1–3, 175–183. https://doi.org/10.1016/0022-3093(80)90019-8

Schreiber, H. D. (1987). An Electrochemical Series of Redox Couples in Silicate Melts: a review and applications to geochemistry. *Journal of Geophysical Research*, *92*, 9225–9232. https://doi.org/10.1029/JB092iB09p09225

Schreiber, H. D., Balazs, G. B., Shaffer, A. P., & Jamison, P. L. (1982). Iron metal production in silicate melts through the direct reduction of Fe(II) by Ti(III), Cr(II), and Eu(II). *Geochimica et Cosmochimica Acta*, *46*, 10, 1891–1901. https://doi.org/10.1016/0016-7037(82)90127-2

Schreiber, H. D., Kochanowski, B. K., Schreiber, C. W., Morgan, A. B., Coolbaugh, M. T., & Dunlap, T. G. (1994). Compositional dependence of redox equilibria in sodium silicate glasses. *Journal of Non-Crystalline Solids*, *177*, 340–346. https://doi.org/10.1016/0022-3093(94)90548-7

Schreiber, H. D., Lauer, H. V., & Thanyasiri, T. (1980). The redox state of cerium in basaltic magmas: an experimental study of iron-cerium interactions in silicate melts. *Geochimica et Cosmochimica Acta*, *44*, 10, 1599–1612. https://doi.org/10.1016/0016-7037(80)90120-9

Schreiber, H. D., Merkel, R. C., Schreiber, V. L., & Balazs, G. B. (1987). Mutual interactions of redox couples via electron exchange in silicate melts: Models for geochemical melt systems. *Journal of Geophysical Research*, *92*, B9, 9233. https://doi.org/10.1029/JB092iB09p09233

Schreiber, H. D., Wilk Jr, N. R., & Schreiber, C. W. (1999). A comprehensive electromotive force series of redox couples in soda–lime–silicate glass. *Journal of Non-Crystalline Solids*, *253*, 1–3, 68–75. https://doi.org/10.1016/S0022-3093(99)00344-0

Shannon, R. D. (1976). Revised effective ionic radii and systematic studies of interatomic distances in halides and chalcogenides. *Acta Crystallographica Section A*, *32*, 5, 751–767. https://doi.org/10.1107/S0567739476001551

Shaw, D. M. (2006). *Trace elements in magmas : a theoretical treatment*. Cambridge University Press.

Shearer, C. K., Papike, J. J., Burger, P. V., Sutton, S. R., McCubbin, F. M., & Newville, M. (2011). Direct determination of europium valence state by XANES in extraterrestrial merrillite: Implications for REE crystal chemistry and martian magmatism. *American Mineralogist*, *96*, 8–9, 1418–1421. https://doi.org/10.2138/am.2011.3860

Shearer, C. K., Papike, J. J., & Karner, J. M. (2006). Pyroxene europium valence oxybarometer: Effects of pyroxene composition, melt composition, and crystallization kinetics. *American Mineralogist*, *91*, 10, 1565–1573. https://doi.org/10.2138/am.2006.2098

Smythe, D. J., & Brenan, J. M. (2015). Cerium oxidation state in silicate melts: Combined fO2, temperature and compositional effects. *Geochimica et Cosmochimica Acta*, *170*, 173–187. https://doi.org/10.1016/j.gca.2015.07.016

Smythe, D. J., & Brenan, J. M. (2016). Magmatic oxygen fugacity estimated using zircon-melt partitioning of cerium. *Earth and Planetary Science Letters*, *453*. Elsevier. https://doi.org/10.1016/j.epsl.2016.08.013

Smythe, D. J., Brenan, J. M., Bennett, N. R., Regier, T., & Henderson, G. S. (2013). Quantitative determination of cerium oxidation states in alkali-aluminosilicate glasses using M4,5-edge XANES. *Journal of Non-Crystalline Solids*, *378*, 258–264. https://doi.org/10.1016/J.JNONCRYSOL.2013.07.017

Sutton, S. R. R., Karner, J., Papike, J., Delaney, J. S. S., Shearer, C., Newville, M., et al. (2005). Vanadium K edge XANES of synthetic and natural basaltic glasses and application to microscale oxygen barometry. *Geochimica et Cosmochimica Acta*, *69*, 9, 2333–2348. https://doi.org/10.1016/j.gca.2004.10.013

Takahashi, Y., Kolonin, G. R., Shironosova, G. P., Kupriyanova, I. I., Uruga, T., & Shimizu, H. (2005). Determination of the Eu(II)/Eu(III) ratios in minerals by X-ray absorption near-edge structure (XANES) and its application to hydrothermal deposits. *Mineralogical Magazine*, *69*, 2, 179–190. https://doi.org/10.1180/0026461056920245

Takahashi, Y., Sakami, H., & Nomura, M. (2002). Determination of the oxidation state of cerium in rocks by Ce LIII-edge X-ray absorption near-edge structure spectroscopy. *Analytica Chimica Acta*, *468*, 2, 345–354. https://doi.org/10.1016/S0003-2670(02)00709-2

Tanaka, T., Yoshida, T., Yoshida, S., Baba, T., & Ono, Y. (1995). XANES study of Eu species encapsulated in potassium Y-type zeolite. *Physica B: Condensed Matter*, *208–209*, 687–688. https://doi.org/10.1016/0921-4526(94)00790-3

Tostevin, R., Shields, G. A., Tarbuck, G. M., He, T., Clarkson, M. O., & Wood, R. A. (2016). Effective use of cerium anomalies as a redox proxy in carbonate-dominated marine settings. *Chemical Geology*, *438*, 146–162. https://doi.org/10.1016/J.CHEMGEO.2016.06.027

Trail, D., Watson, E. B., & Tailby, N. D. (2011). The oxidation state of Hadean magmas and implications for early Earth's atmosphere. *Nature*, *480*, 7375, 79–82. https://doi.org/10.1038/nature10655

Treuil, M, & Joron, J. L. (1975). Utilisation des elements hygromagmatophiles pour la simplification de la modélisation quantitative des processus magmatiques: exemples de l'Afar et de la dorsale médio-atlantique. *Società Italiana Mineralogia e Petrologia*, *31*, 1, 125–174.

Treuil, M., Joron, J.-L., Jaffrezic, H., Villemant, B., & Calas, G. (1979). Géochimie des éléments hygromagmatophiles, coefficients de partage minéraux /liquides et propriétés structurales de ces éléments dans les liquides magmatiques. *Bulletin de Minéralogie*, *102*, 4, 402–409. https://doi.org/10.3406/bulmi.1979.7336

Treuil, M., & Varet, J. (1973). Criteres volcanologiques, petrologiques et geochimiques de la genese et de la differenciation des magmas basaltiques; exemple de l'Afar. *Bulletin de La Societe Geologique de France*, *S7-XV*, 5–6, 506–540. https://doi.org/10.2113/gssgfbull.S7-XV.5-6.506

Ueda, K., Shimizu, Y., Nagamizu, K., Matsuo, M., & Honma, T. (2017). Luminescence and Valence of Tb Ions in Alkaline Earth Stannates and Zirconates Examined by X-ray Absorption Fine Structures. *Inorganic Chemistry*, *56*, 20, 12625–12630. https://doi.org/10.1021/acs.inorgchem.7b02165

Virgo, D., Seifert, F. A., & Mysen, B. O. (1981). The oxidation state of europium in albite and alkali-earth silicate glasses. *Carnegie Institute of Washington Yearbook*, *80*, 313–316.

Wadhwa, M. (2008). Redox Conditions on Small Bodies, the Moon and Mars. *Reviews in Mineralogy and Geochemistry*, *68*, 1, 493–510. https://doi.org/10.2138/rmg.2008.68.17

Wang, C., Peng, M., Jiang, N., Jiang, X., Zhao, C., & Qiu, J. (2007). Tuning the Eu luminescence in glass materials synthesized in air by adjusting glass compositions. *Materials Letters*, *61*, 17, 3608–3611. https://doi.org/10.1016/j.matlet.2006.11.133

Weill, D. F. F., & Drake, M. J. J. (1973). Europium anomaly in plagioclase feldspar: experimental results and semiquantitative model. *Science*, *180*, 4090, 1059–1060. https://doi.org/10.1126/science.180.4090.1059

White, W. M. (2013). *Geochemistry*. John Wiley & Sons.

Wilke, M., & Behrens, H. (1999). The dependence of the partitioning of iron and europium between plagioclase and hydrous tonalitic melt on oxygen fugacity. *Contributions to Mineralogy and Petrology*, *137*, 1–2, 102–114. https://doi.org/10.1007/s004100050585